PSFC/JA-12-37

Heat-flux footprints for I-mode and EDA H-mode plasmas on Alcator C-Mod

J.L. Terry, B. LaBombard, D. Brunner, J. W. Hughes,
M.L. Reinke, and D.G. Whyte

November 2012

Plasma Science and Fusion Center
Massachusetts Institute of Technology
Cambridge MA 02139 USA

This work was supported by the U.S. Department of Energy Coop. Agreement DE-FC02-99-ER54512. Reproduction, translation, publication, use and disposal, in whole or in part, by or for the United States government is permitted.

Submitted for publication to the *Journal of Nuclear Materials.*

Heat-flux footprints for I-mode and EDA H-mode plasmas on Alcator C-Mod

J.L. Terry*, B. LaBombard, D. Brunner, J. W. Hughes, M.L. Reinke, and D.G. Whyte

Plasma Science and Fusion Center, MIT, Cambridge, MA, USA 02139

Abstract

IR thermography is used to measure the heat flux footprints on C-Mod's outer target in I-mode and EDA H-mode plasmas. The footprint profiles are fit to a function with a simple physical interpretation. The fit parameter that is sensitive to the power decay length into the SOL, λ_{SOL}, is ~1-3x larger in I-modes than in H-modes at similar plasma current, which is the dominant dependence for the H-mode λ_{SOL}. In contrast, the fit parameter sensitive to transport into the private-flux-zone along the divertor leg is somewhat smaller in I-mode than in H-mode, but otherwise displays no obvious dependence on I_p, B_t, or stored energy. A third measure of the footprint width, the "integral width", is not significantly different between H- and I-modes. Also discussed are significant differences in the global power flows of the H-modes with "favorable" ∇B drift direction and those of the I-modes with "unfavorable" ∇B drift direction.

PACS: 52.55.Rk, 52.55.Fa, 52.25Fi, 52.70.Kz

**Corresponding Author Address:* 175 Albany St., Cambridge, MA 02319 USA

**Corresponding Author E-mail:* terry@psfc.mit.edu

Presenting Author: James L. Terry

Presenting Author E-mail: terry@psfc.mit.edu

I. Introduction

Acceptable power handling is one of the primary functions - and most challenging problems - for a tokamak divertor. Recent work [1-6] has focused on measurements of the heat-flux "footprints" on divertor surfaces and heat-flux widths during H-mode confinement in various tokamaks (Alcator C-Mod, AUG, DIII-D, JET, and NSTX). This interest is due in large part to the desire to understand the physics that sets the heat-flux widths and to predict them in ITER [2, 5, 7, 6], since they will play a crucial role in determining the difficulty of an acceptable solution for power handling in the ITER divertor. These multi-machine studies indicate that the width scales inversely with the poloidal field strength, B_{pol}, which when extrapolated to ITER yields a ~1mm width [2, 5, 6]. Widths this small would substantially increase the difficulty of finding a divertor solution. Similar width values are obtained when the heuristic, drift-based model of [7] is extrapolated to ITER. Whether such a small width can be sustained on ITER is without violating other constraints is currently being studied [8].

IR thermography was used as the common measurement technique on these different devices, and the resulting footprints are being fit to functions of the same form so that differences can be compared directly [5, 6]. An especially useful functional form that has valuable physical interpretation has been recently proposed by Eich [2] and is now being used for multi-machine comparisons. This form fits the heat-flux footprints to a function that yields a measure of the perpendicular transport into the common-flux region, λ_{SOL} (the λ_q parameter in [2]), as well as a measure of the transport into the private flux zone (PFZ) along the outer leg of the divertor, w_{PFZ} (the *S* parameter in [2]). Another measure of more direct relevance to the power handling requirement is the integral power width [9], λ_{Int}, which relates the peak heat load to the total power incident on the target, i.e. $\lambda_{Int} = \int q_{DIV} 2\pi R\, dr\, f^{-1} \,/ q_{DIV}{}^{peak}\, 2\pi R$, where f is the midplane-to-divertor magnetic flux

expansion. In this work, these measures have been used to parameterize footprints from C-Mod's Enhanced-D-Alpha (EDA) H-mode and I-mode plasmas.

The I-mode plasmas are of particular interest because of their attractive confinement features [10, 11] and because the edge heat and particle transport are more de-coupled than in H-mode, allowing for a large temperature pedestal and high energy-confinement (H_{98}<1.2) *without* a density pedestal and without ELMs regulating the edge pressure. Thus the edge profile gradient-scale-lengths for T_e are similar in I-mode and H-mode, while the edge gradient-scale-lengths for n_e are different, with $L_{ne}^{\text{I-mode, ped}} \sim 10 x L_{ne}^{\text{H-mode,ped}}$ [10]. We compare the I-mode and H-mode heat-flux footprints, both as part of the evaluation of the I-mode regime and for insight into the physics of what determines the widths. Because characteristics of the I-mode confinement regime are not necessarily widely known, we list three additional characteristics to supplement those just mentioned: 1) I-modes are typically obtained in the "unfavorable" ∇B drift configuration, so as to stay below the H-mode power threshold and obtain the widest "power window" for maintaining I-mode (to date I-modes have been sustained at powers ~1.8x the L-to-I-mode threshold); 2) I-mode is stationary, having been maintained on C-Mod with steady conditions for >10 energy confinement times, and 3) to date, I-mode confinement scales roughly as $P_{in}^{-0.3}$, i.e. it falls less strongly with power than for H- and L-mode.

II. Experimental details and analyses

Alcator C-Mod is a compact high field tokamak that uses auxiliary ICRF heating. At the bottom of the device is a closed divertor with solid Mo tile targets which receive parallel heat-fluxes up to ~500 MW/m^2. Heat-flux measurements are made on an instrumented section of the outer target of that closed divertor. Imaging IR thermography, calibrated after each shot using embedded thermocouples, is used in the high heat flux cases of interest here to measure the time-histories of surface temperature profiles. These measurements, combined

with the poloidal and radial geometry and thermal properties of the Mo target tiles, are analyzed to produce profiles of heat flux incident on the tiles using the 2D heat flux code QFLUX2D. The thermography and heat flux code are described in more detail in [12, 4]. A typical heat flux profile from an I-mode plasma is shown in Fig.1. Of note are: 1) the abscissa, ρ, is the distance outside the Last Closed Flux Surface (LCFS) when magnetically-mapped from the target to the outboard midplane[1], 2) the ordinate is the parallel heat-flux at a given ρ as inferred using knowledge of the surface heat flux and field line angle of incidence, 3) the peak values of $q_{||}$ are typically ~200-500 MW/m^2 in unseeded high performance plasmas, 4) there is always a far-SOL "tail" in the profile with roughly constant heat flux, and 5) the heat flux decay into the PFZ is steeper than the decay into the common SOL. In the case shown, the peak in the target heat flux is not perfectly aligned with the EFIT-located strike point. We attribute that to errors in the equilibrium reconstruction of the strike-point location and find that shifts of < 2mm typically bring the two into alignment.

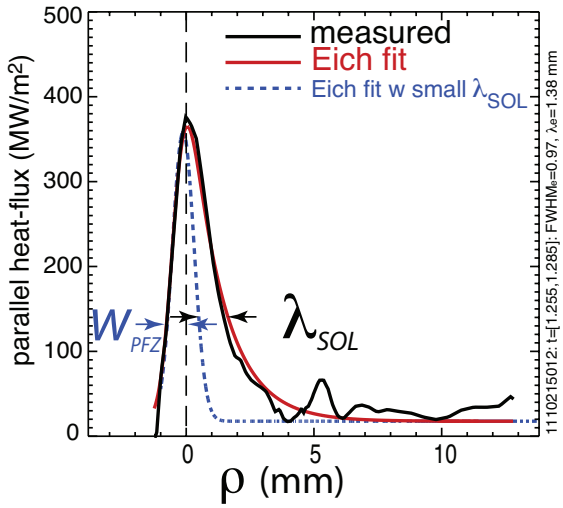

Figure 1. *(color online) Typical parallel heat flux profile on the outer target from an I-mode plasma. The profile has been magnetically mapped to the outboard midplane and shifted by 1.6 mm from the EFIT value in order to align the peak with ρ=0. The Eich fit to the profile (λ_{SOL}=1.38 mm, w_{PFZ}=0.58 mm) is shown in red. The blue dashed curve shows the effect of a small value of λ_{SOL} (0.1 mm) with w_{PFZ} held constant to still match the profile in the PFZ. λ_{SOL} is used to describe the profile fall-off in the common-flux region. The heat-flux profile "tail" is a typical feature on C-Mod.*

Finally, there exist a few shots in which the strike-point was swept over operational Langmuir probes and/or fast-response surface thermocouples [13], thereby allowing comparison of the common-flux part of heat flux profiles measured in this way with those

[1] PFZ regions, which do not map to the midplane, are assigned ρ values equal to the ρ value of closed flux surfaces in the core plasma having the same value of poloidal flux.

measured using thermography. In those cases, the IR profile is somewhat broader than that from the probe with essentially the same peak heat flux, while the IR profile is from 1-3x broader than that inferred from the surface TC. The reasons for this are being investigated. In this study only profiles from the IR thermography will be compared.

The target heat flux profiles are fit using a physics-based parameterization due to Eich [2] that convolves a Gaussian with a decaying exponential function:

$$q_{||} = \frac{q_{||,0}}{N\sqrt{\pi w_{PFZ}{}^2}} \int_0^\infty e^{-s_0/\lambda_{SOL}} e^{-(s-s_0)^2/w_{PFZ}{}^2} ds_0 + q_{bkg} \qquad \text{(Eq. 1)}$$

where $q_{||,0}$ is the peak parallel heat flux, q_{bkg} is a "background" heat flux that will represent the observed "tails", λ_{SOL} describes the profile broadening due to perpendicular transport into the SOL occurring before entering the divertor, and w_{PFZ} represents the competition between perpendicular and parallel transport that allows for the spreading of the footprint into the PFZ along the outer divertor leg, s is the profile coordinate, defined such that the strike point location is $s=0$. This parameterization is illustrated in Fig. 1 by the red and blue-dashed curves, where the red curve is the best fit to the measured profile (λ_{SOL}=1.38 mm, w_{PFZ} =0.58 mm), while the dashed curve, with the same w_{PFZ}, but a much smaller λ_{SOL}, is used to illustrate the fit to the PFZ profile and to show the need for a larger λ_{SOL} in order to follow the fall-off of the measured profile in the common-flux region. We examine the scaling of these heat-flux-profile-fitting parameters as well as the values of λ_{Int} in the next section.

III. Scaling of heat-flux footprints in EDA H-mode and in I-mode

1. EDA H-mode results

LaBombard, et al. [4] described the dependencies of C-Mod heat-flux widths in EDA H-modes and Ohmic L-modes. These plasmas were made in a LSN configuration with the B_t direction such that the ∇B drift direction was favorable for H-mode (the "normal" direction). For that work, target heat flux widths were characterized both by an e-folding length on the

common-flux side of the profile, $\lambda_{EFOLD} \rightarrow \lambda_{SOL}$ for $w_{PFZ} \rightarrow 0$, and by the FWHM of the main peak of the footprint, $FWHM \approx 1.66 w_{PFZ} + \ln 2 \lambda_{SOL}$. Those width parameters showed a general decrease with increased stored energy. A I_p^{-1} dependence (also found in other devices) was found for λ_{EFOLD} of plasmas selected for having high values of stored energy per unit I_p. No significant dependencies were found in the λ_{EFOLD}, λ_{Int}, or FWHM measures for power in the SOL ($P_{SOL}=P_{in}-P_{rad}$), B_t, or full connection length. For the present work, these same discharges have been re-analyzed using the more elaborate Eich parameterization with λ_{SOL} and w_{PFZ}. Results vs I_p are shown in Fig. 2 as the blue triangles. *The width dependence on I_p is found to be in λ_{SOL}* (roughly $\propto 1/I_p$ for the plasmas selected for high stored energy per unit I_p – Fig. 2a), while w_{PFZ} shows no consistent dependence either on I_p (Fig. 2b), B_t, or stored energy. Finally, the dependence of the integral width, λ_{Int}, vs I_p is shown in Fig. 3 for the same discharges. In this important power-handling measure, the I_p dependence is much reduced due to the combined effect of the profile "tail" and the Gaussian width, w_{PFZ}.

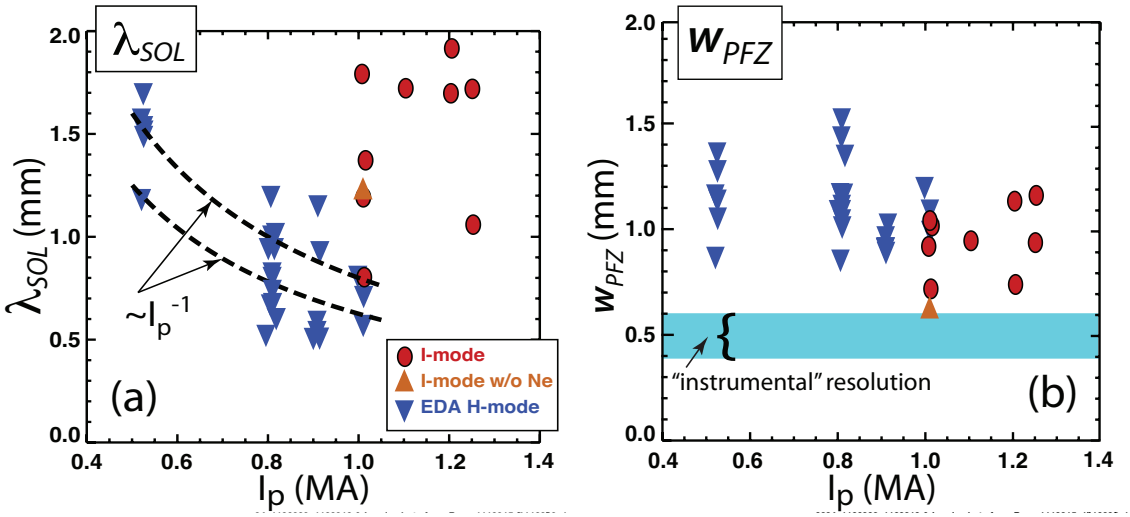

Figure 2. *(color online) (a) Comparison of the values of the fit parameter λ_{SOL} vs I_p for the heat flux profiles of EDA H-modes and I-modes. These points are from discharges selected for having high thermal energy per unit I_p. (b) Comparison of the values of the fit parameter w_{PFZ} vs I_p for the same discharges. The blue band indicates the estimate for minimum resolution of the measurement/analysis.*

2. I-mode results

I-mode confinement discharges are more readily produced with the ∇B drift in the "unfavorable" direction since this raises the H-mode threshold and widens the power window available for I-mode. In order to put the heat flux footprint onto the lower *instrumented* target with unfavorable drift, "reversed" field is required. While this leads to quite different power sharing between inboard and outboard targets (discussed below), it also means that there are fewer I-mode LSN discharges and that the parameter space for which I-mode footprint data exist is restricted compared that for H-mode. In particular, scans of I_p and B_t dedicated to footprint measurements do not exist for I-mode; measurements exist only for the current range $1.0 < I_p < 1.25$ MA with $5.1 < |B_t| < 5.7$ T. Nonetheless, the measure of the footprint decay into the common SOL, λ_{SOL}, for I-modes is observed to be 1-3x larger when compared to those of H-modes. This is apparent in Fig. 2a where λ_{SOL} values for the I-mode points are compared with those of H-mode. The scatter in the values and the restricted I_p range for the I-modes make it impossible to discern any scaling of λ_{SOL} with I_p. The observation that λ_{SOL} is similar to or larger in I-mode compared to H-mode is important for insight into the physics responsible for setting the width (Sect. IV), but does not mean that the I-mode power handling requirements (relative to H-mode) are reduced by the same factor. This is apparent when the integral widths, λ_{Int}, are compared (Fig. 3); the values of λ_{Int} in I-mode are not statistically different from those of the H-modes. The presence of the profile "tail" and the somewhat smaller I-mode values for w_{PFZ} (Fig. 2b) reduce the effect of the larger λ_{SOL} width. As shown in Fig. 2b, the average w_{PFZ} for the I-mode points is ~20% smaller than that for H-mode. At

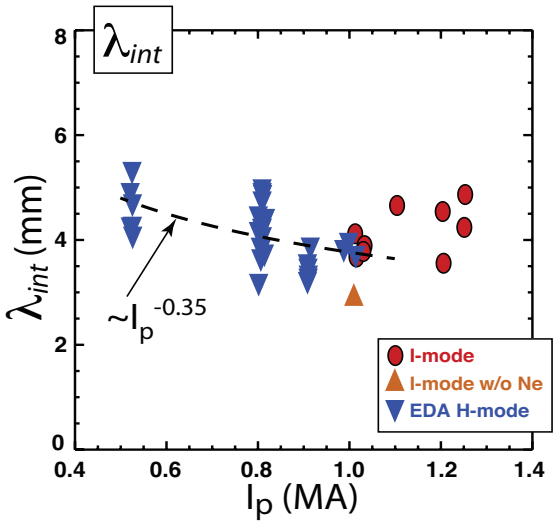

Figure 3. *(color online) Comparison of the footprint "integral widths", λ_{Int}, vs I_p for the same EDA H-modes and I-modes of Fig. 2.*

present we can only speculate about reasons for this difference, relating it to possible differences in drifts due to the "reversed" field configuration of the I-mode discharges. It may be related to whatever is causing differences in w_{PFZ} found for different Asdex-Upgrade divertor geometries [5]. On C-Mod, w_{PFZ} exhibits no obvious dependence on I_p or stored energy. Also shown in Fig. 2b is a shaded band that represents the "instrumental resolution" for w_{PFZ}, which we believe represents the system's minimum resolution for w_{PFZ}. (This has been evaluated using actual thermography images that were run though the QFLUX2D analysis.) Thus we believe that, except for possibly the lowest cases, the values of w_{PFZ} shown in Figs. 2b have a *physics* basis and not an instrumental one[2].

We now examine the global "power-flow" characteristics of I-mode in more detail. The range of input power was roughly the same in the I-mode and H-mode plasmas studied here. However, because the impurity transport is L-mode-like in I-mode [10], the "main chamber" power radiated from I-mode plasmas is typically significantly less than or at most similar to that radiated from EDA H-modes ($P_{rad}^{H\text{-}mode} \sim 1\text{-}3 x P_{rad}^{I\text{-}mode}$), and the power conducted into the SOL, P_{SOL}, is typically larger in these I-mode plasmas. In fact we observe that roughly $P_{SOL}^{I\text{-}mode} \sim 1\text{-}3 x P_{SOL}^{H\text{-}mode}$, which increases the divertor power-handling loads for I-mode plasmas. For the "reversed-field" configuration of these I-modes, however, the power-sharing between inner and outer targets is significantly changed [14] such that the *inner* target receives roughly 1.5x to 3x times more shot-integrated energy than is received on the outer target. For the "normal-field" H-modes in this study, the energy asymmetry is 1x to 2x greater on the outer target. The end result of this set of differences between the H- and I-mode "power-flows" and footprints is that the peak heat-fluxes on the *outer* target, as well as the total powers on the outer target, are roughly the same for the plasmas compared here. The

[2] This assumes that rapid strike-point oscillation from some unknown source or a stochastic magnetic region associated with the x-point zone is not smearing the profile into the PFZ, since that would not be accounted for in the "instrumental resolution" estimate.

peak heat fluxes are shown in Fig. 4. However, this is not true for the inner target, where power handling is a much bigger issue in these I-modes. Indeed, small amounts of neon were seeded into all but one of these I-modes in order to reduce target heat loads. Low-Z impurity seeding into I-modes is far better tolerated by I-modes (i.e. is without significant negative effects) as compared to seeding into H-modes because of the L-mode-like impurity confinement of I-mode.

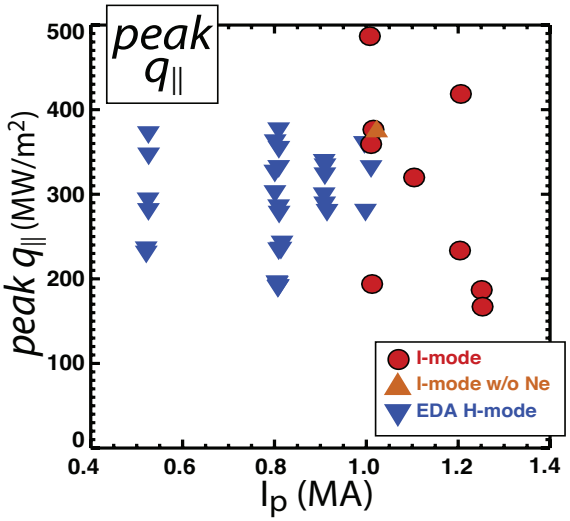

Figure 4. (color online) Comparison of the outer target's peak parallel heat flux, $q_{||}^{peak}$, vs I_p for the same EDA H-modes and I-modes of Fig. 2.

Another I-mode/H-mode difference is significantly lower collisionality in the I-mode. This results in "sheath-limited" conditions at the inner and outer targets in I-mode, compared to "high-recycling" conditions at the outer target in H-mode. Additionally, the parallel power flow in the I-mode SOL is most likely "flux-limited"[15], with $\nu^*_{e,SOL}=L_{||}/\lambda_{ee}$=5-50 << that of C-Mod's H-modes.

Finally, for completeness, we have examined whether the low-Z impurity seeding used in most of the I-mode plasmas might cause a systematic broadening of the profile and might result in larger values for λ_{SOL} in the I-mode cases. While we cannot unequivocally eliminate this possibility, we believe it to be highly unlikely since 1) λ_{SOL} for the single non-seeded I-mode is not significantly different than λ_{SOL} for the seeded I-modes, 2) the outer divertor was sheath-limited and fully attached in all I-modes, 3) (as mentioned above) the total radiated power was similar or *smaller* in the I-mode plasmas, and 4) the powers on the outer target were in the same range, 0.5<P_{odiv}<1.3 MW for the H-modes and I-modes considered here.

IV. Discussion

We have found that λ_{SOL} in I-modes with $1 \le I_p \le 1.25$ MA is ~1-3x larger than in EDA H-mode at I_p ~1MA. The obvious question is: what is different about the I-mode plasmas that would result in SOL heat flux widths that are larger than in H-modes? We hypothesize that it is related to whatever relaxes the density pedestal in I-mode. As mentioned previously, the tight coupling between particle and energy transport in the H-mode pedestal is much reduced in I-mode, since its edge density profiles are L-mode-like. Previous work on footprint widths of C-Mod's *Ohmic* L-modes[4] showed a clear correlation between the pressure decay length in the upstream SOL, L_{nTe}, and the heat-flux width, both scaling as I_p^{-1}. The new I-mode observations are qualitatively consistent with this picture since L_{nTe} is increased in I-mode as compared to H-mode. Further quantitative comparisons of L_{nTe} and λ_{SOL} require a detailed analysis of the upstream scale-lengths of T_e, T_i and n_e, an analysis that is outside the scope of this paper.

In summary, we find that, for EDA H-modes with the high stored energy per unit I_p, λ_{SOL} values for footprints magnetically mapped to the midplane are in the 0.5-1.7 mm range and exhibit an approximate inverse scaling with I_p. In the I-modes studied, λ_{SOL} ~0.8-2 mm for $1 \le I_p \le 1.25$ MA and is ~1-3x the H-mode values in plasmas in a similar current range. This difference is qualitatively consistent with the correlation of λ_{SOL} with upstream pressure decay length that was found for Ohmic L-modes in C-Mod [4]. In contrast, the integral width, λ_{int}, shows no significant difference between I- and H-modes The w_{PFZ} parameter appears to vary between (normal-field-direction) H-mode and (reversed-field-direction) I-mode plasmas, but shows no obvious dependence either on plasma current or stored energy, with values ranging between 0.6 and 1.5 mm in C-Mod.

Acknowledgement

We would like to acknowledge valuable discussions with Thomas Eich of IPP Garching and Michael Makowski at GA (DIII-D). This work is supported by DoE Coop. Agreement DE-FC02-99-ER54512.

References

[1] Ahn, J.W., Maingi, R., Boedo, J.A., and Soukhanovskii, V., Journal of Nuclear Materials **390-391** (2009) 421.
[2] Eich, T., et al., Physical Review Letters **107** (2011) 215001.
[3] Eich, T., et al., Journal of Nuclear Materials **415** (2011) S856.
[4] LaBombard, B., et al., Physics of Plasmas **18** (2011) 056104.
[5] Eich, T., this conference (paper I7) (2012.
[6] Makowski, M.A., et al., Physics of Plasmas **19** (2012) 056122 (9 pp.).
[7] Goldston, R.J., Nuclear Fusion **52** (2012) 013009 (7 pp.).
[8] Whyte, D.G., this conference (paper P1-037) (2012.
[9] Loarte, A., et al., Journal of Nuclear Materials **266-269** (1999) 587.
[10] Whyte, D.G., et al., Nuclear Fusion **50** (2010) 105005 (11 pp.).
[11] Hubbard, A.E., et al., Physics of Plasmas **18** (2011) 056115 (9 pp.).
[12] Terry, J.L., Labombard, B., Brunner, D., Payne, J., and Wurden, G.A., Review of Scientific Instruments **81** (2010) 10E513 (4 pp.).
[13] Brunner, D. and LaBombard, B., Review of Scientific Instruments **83** (2012) 033501.
[14] Pitts, R.A., et al., Journal of Nuclear Materials **337-339** (2005) 146.
[15] Stangeby, P.C., Canik, J.M., and Whyte, D.G., Nuclear Fusion **50** (2010) 125003 (12 pp.).